Langmuir
Article
pubs.acs.org/Langmuir

The Actual Dielectric Response Function for a Colloidal Suspension of Spherical Particles

B. H. Bradshaw-Hajek,[†] S. J. Miklavcic,*[,†,‡] and L. R. White[†]

[†]*School of Mathematics and Statistics, University of South Australia, Mawson Lakes, SA 5095, Australia, and* [‡]*Department of Science and Technology, University of Linköping, S-601 74 Norrköping, Sweden*

Received December 17, 2009. Revised Manuscript Received March 28, 2010

In this paper, we present a theoretical analysis of the dielectric response of a dense suspension of spherical colloidal particles based on a self-consistent cell model. Particular attention is paid to (a) the relationship between the dielectric response and the conductivity response and (b) the connection between the real and imaginary parts of these responses based on the Kramers−Kronig relations. We have thus clarified the analysis of Carrique et al. (Carrique, F.; Criado, C.; Delgado, A. V. *J. Colloid Interface Sci.* **1993**, *156*, 117). We have shown that both the conduction and displacement current components are complex quantities with both real and imaginary parts being frequency dependent. The dielectric response exhibits characteristics of two relaxation phenomena: the Maxwell−Wagner and the α-relaxations, with the imaginary part being the more sensitive instrument. The inverse Fourier transform of the simulated dielectric response is compared with a phenomenological, two-exponential response function with good agreement obtained. The two fitted decay times also compare well with times extracted from the explicit simulations.

1. Introduction

The measurement of the high frequency ($\omega \sim 10^4-10^7$) dielectric response of a colloidal suspension $\varepsilon(\omega) = \varepsilon'(\omega) + i\varepsilon''(\omega)$ is a somewhat neglected technique for probing the state of charge of the particle surface. The advantages of the technique are its noninvasive nature and the simultaneous measurement of two experimental properties (real and imaginary parts of the conductivity) as functions of frequency over an extensive experimental range which encompasses the important double layer relaxation processes for particles of typical colloidal dimension (particle radius $a \sim 100$ nm). The neglect may have its origins in the historical focus on the low frequency region ($\omega \sim 10^2-10^4$) where nevertheless experimental artifacts such as electrode impedance were difficult to extract from the data.[1] (Note that electrode impedance is negligible at high frequencies[2] and the problem of lead inductance at high frequency can be effectively minimized by clever cell design.[3])

In addition, the small imaginary part of the conductivity at low frequencies was difficult to measure accurately in the presence of a large real part. For this reason, measurement was restricted to suspensions of low conductivity to facilitate the separation. This difficulty is not present at high frequency, since the real and imaginary parts are comparable in this range.

Historically, the theory by which these properties may be interpreted in terms of the state of surface charge was not completely developed, especially for the low κa regions to which the technique was confined. The theory of DeLacey and White[4] enabled the interpretation of the low κa region for all ζ potential values but was itself restricted to frequencies $\omega \leq 10^6$ (due to the neglect of fluid inertia) and low volume fraction ($\phi \ll 0.1$) suspensions. The later theory of Mangelsdorf and White[5] removed the frequency restriction in the theory but was subject to numerical difficulties at frequencies $\omega \sim 10^7$ while still being restricted to dilute suspensions. Recently, the advent of cell model theories[1,6−13] and the use of stiff differential equation solvers[14−17] have removed both frequency and volume fraction restrictions.

Thus, it would seem that, in our brave new world, there should be no impediment to the widespread use of high frequency dielectric spectroscopy in colloid science, given the cost of impedance bridges relative to electroacoustic devices. Indeed, dielectric measurements across a wide range of frequencies that encompasses both relaxations would provide more information about the system.[18,19]

The complex conductivity of a suspension of colloidal particles as measured by its response to an applied alternating electric field may be written

$$K^*(\omega) = K^*_{\mathrm{cond}}(\omega) + K^*_{\mathrm{disp}}(\omega) \qquad (1)$$

(1) Carrique, F.; Arroyo, F. J.; Jimenez, M. L.; Delgado, A. V. *J. Chem. Phys.* **2003**, *118*, 1945.
(2) Hollingsworth, A. D.; Saville, D. A. *J. Colloid Interface Sci.* **2004**, *272*, 235.
(3) Midmore, B. R.; Hunter, R. J.; O'Brien, R. W. *J. Colloid Interface Sci.* **1987**, *120*, 210.
(4) DeLacey, E. H. B.; White, L. R. *J. Chem. Soc., Faraday Trans. 2* **1981**, *77*, 2007.
(5) Mangelsdorf, C. S.; White, L. R. *J. Chem. Soc., Faraday Trans.* **1992**, *88*, 3567.
(6) Ohshima, H. *J. Colloid Interface Sci.* **1997**, *195*, 137.
(7) Ohshima, H. *J. Colloid Interface Sci.* **1997**, *188*, 481.
(8) Dukhin, A. S.; Shilov, V. N.; Borkovskaya, Y. B. *Langmuir* **1999**, *15*, 3452.
(9) Dukhin, A. S.; Shilov, V. N.; Ohshima, H.; Goetz, P. J. *Langmuir* **1999**, *15*, 6692.
(10) Lee, E.; Chu, J. W.; Hsu, J. *J. Colloid Interface Sci.* **1999**, *209*, 481.
(11) Hsu, J. P.; Lee, E.; Yen, F. Y. *J. Chem. Phys.* **2000**, *112*, 6404.
(12) Carrique, F.; Arroyo, F. J.; Delgado, A. V. *J. Colloid Interface Sci.* **2001**, *243*, 351.
(13) Zholkovskij, E. K.; Masliyah, J. H.; Shilov, V. N.; Bhattacharjee, S. *J. Colloid Interface Sci.* **2007**, *133−134*, 279.
(14) Ahualli, S.; Delgado, A.; Miklavcic, S.; White, L. R. *Langmuir* **2006**, *22*, 7041.
(15) Ahualli, S.; Delgado, A.; Miklavcic, S.; White, L. R. *J. Colloid Interface Sci.* **2007**, *309*, 342.
(16) Bradshaw-Hajek, B. H.; Miklavcic, S. J.; White, L. R. *Langmuir* **2008**, *24*, 4512.
(17) Bradshaw-Hajek, B. H.; Miklavcic, S. J.; White, L. R. *Langmuir* **2009**, *25*, 1961.
(18) Feldman, Y.; Skodvin, T.; Sjoblom, J. In *Encyclopedic handbook of emulsion technology*; Sjoblom, J., Ed.; Marcel Dekker: New York, 2001; Chapter 6, p 109.
(19) Grosse, C. In *Interfacial electrokinetics and electrophoresis*; Delgado, A. V., Ed.; Surfactant Science Series; Marcel Dekker: New York, 2002; Vol. *106*, Chapter 11, p 277.

The first term is the conduction contribution due to the ion convection current and can be written as

$$K^*_{\mathrm{cond}}(\omega) = K'_{\mathrm{cond}}(\omega) + iK''_{\mathrm{cond}}(\omega)$$

The second term is the displacement contribution arising from the polarization of the particles, their double layers, and the medium, and this serves to define the effective dielectric response function of the suspension, $\varepsilon(\omega)$, as

$$K^*_{\mathrm{disp}}(\omega) = -i\omega\varepsilon_0\varepsilon(\omega) = \omega\varepsilon_0(\varepsilon''(\omega) - i\varepsilon'(\omega))$$

The complex conductivity (eq 1) may then be written as

$$K^*(\omega) = \left[K'_{\mathrm{cond}}(\omega) + \omega\varepsilon_0\varepsilon''(\omega)\right] + i\left[K''_{\mathrm{cond}}(\omega) - \omega\varepsilon_0\varepsilon'(\omega)\right] \tag{2}$$

Both $K^*_{\mathrm{cond}}(\omega)$ and the suspension dielectric response function $\varepsilon(\omega)$ are a priori functions of particle volume fraction ϕ. Note that we use the physics convention that the Fourier component of a time varying function $f(t)$ is $f_\omega\, e^{-i\omega t}$ so that the sign of imaginary terms will differ from those in ref 20.

Historically,[1,4,16−21] it has been assumed that $K''_{\mathrm{cond}}(\omega)$ is zero. As we shall show, *this assumption is not correct*. In this historical approach, we define

$$\varepsilon'_{\mathrm{Hist}}(\omega) = -\frac{\mathrm{Im}(K^*(\omega))}{\omega\varepsilon_0}$$

and $\varepsilon''(\omega)$ is then constructed using a Kramers−Kronig integration[22]

$$\varepsilon''_{\mathrm{Hist}}(\omega) = \frac{2\omega}{\pi} P \int_0^\infty \mathrm{d}\omega' \frac{\varepsilon'_{\mathrm{Hist}}(\omega') - \varepsilon_\infty}{\omega^2 - \omega'^2}$$

where P denotes the principal value integral and ε_∞ is the high frequency limit

$$\varepsilon_\infty = \lim_{\omega \to \infty} \left[\varepsilon'_{\mathrm{Hist}}(\omega)\right]$$

Hence, $K'_{\mathrm{cond}}(\omega)$ is extracted as

$$K'_{\mathrm{cond}}(\omega) = \mathrm{Re}(K^*(\omega)) - \omega\varepsilon_0\varepsilon''_{\mathrm{Hist}}(\omega) \tag{3}$$

Somewhat surprisingly, the $K'_{\mathrm{cond}}(\omega)$ value obtained by applying this technique to the theoretical $K^*(\omega)$ calculated from the DeLacey−White theory[4] was found to be *frequency independent*, that is, the DC conductivity.[20] This could be taken as a posteriori proof of the initial assumption that the conduction contribution $K^*_{\mathrm{cond}}(\omega)$ was purely real and that the dielectric response so defined was the origin of the true displacement current contribution to the complex conductivity $K^*(\omega)$. In ref 20, the authors demonstrated that the real and imaginary parts of $\varepsilon_{\mathrm{Hist}}(\omega)$ constructed from a DeLacey−White calculation of a theoretical $K^*(\omega)$, when displayed in a Cole−Cole plot, do not correspond to a single relaxation time.

In light of the results of our recent analyses,[17,23] we calculate the actual dielectric response of a suspension and comprehensively describe the two separate contributions to the complex conductivity. Consequently, we clarify the original discussion of Carrique et al.[20] through a rigorous derivation of the dielectric response function and the Kramers−Kronig relationship between its real and imaginary parts. As we show in section 3, the assumption that the imaginary part of the conduction contribution, $K''_{\mathrm{cond}}(\omega)$, is zero is not warranted. We have found that there are two contributions to the complex conductivity, a conduction contribution and a displacement contribution, both of which have frequency dependent real and imaginary parts.

Experimentally, it is not possible to uniquely separate the real and imaginary parts of the conduction contribution, $K^*_{\mathrm{cond}}(\omega)$, or the dielectric response function, $\varepsilon(\omega)$, since impedance methods measure the total conductance of the suspension. It is, however, useful to examine the different contributions to gain a greater understanding of the physical processes occurring.

2. Kramers−Kronig Relationship for the Complex Conductivity

The existence of a Kramers−Kronig relationship between the real and imaginary parts of the complex conductivity is not direct evidence that the real part of the dielectric response has been correctly identified. Any linear response between a real "driving force" $F(t)$ and a real "effect" $R(t)$ in the causal form

$$R(t) = \Delta_\infty F(t) + \int_{-\infty}^{t} \mathrm{d}t'\, D(t-t')\, F(t') \tag{4}$$

(where $D(t)$ is a decay ("memory") function determined by the relaxation processes in the system and the term involving Δ_∞ is the instantaneous response) will possess Fourier components R_ω and F_ω, where

$$R_\omega = \int_{-\infty}^{\infty} \mathrm{d}t\, R(t)\, e^{i\omega t} \quad \text{and} \quad F_\omega = \int_{-\infty}^{\infty} \mathrm{d}t\, F(t)\, e^{i\omega t}$$

with a linear connection

$$R_\omega = \Delta(\omega) F_\omega$$

The "response function" $\Delta(\omega)$ is defined by

$$\Delta(\omega) = \Delta_\infty + \int_0^\infty \mathrm{d}t\, D(t)\, e^{i\omega t} = \Delta'(\omega) + i\Delta''(\omega)$$

Its real and imaginary parts are defined by

$$\Delta'(\omega) = \Delta_\infty + \int_0^\infty \mathrm{d}t \cos\omega t\, D(t)$$

$$\Delta''(\omega) = \int_0^\infty \mathrm{d}t \sin\omega t\, D(t)$$

and hence obey a Kramers−Kronig relationship[22]

$$\Delta'(\omega) - \Delta_\infty = \frac{2}{\pi} P \int_0^\infty \mathrm{d}x \frac{x\Delta''(x)}{x^2 - \omega^2}$$

$$\Delta''(\omega) = \frac{2\omega}{\pi} P \int_0^\infty \mathrm{d}x \frac{\Delta'(x) - \Delta_\infty}{\omega^2 - x^2} \tag{5}$$

(20) Carrique, F.; Criado, C.; Delgado, A. V. *J. Colloid Interface Sci.* **1993**, *156*, 117.
(21) Shilov, V. N.; Delgado, A. V.; González-Cabellero, F.; Grosse, C. *Colloids Surf., A* **2001**, *192*, 253.
(22) Landau, L. D.; Lifshitz, E. M. *Electrodynamics of Continuous Media*; Permagon Press: Oxford, 1960.
(23) Bradshaw-Hajek, B. H.; Miklavcic, S. J.; White, L. R. *Langmuir* **2010**, *26*, 1656.

From its definition, the response function $\Delta(\omega)$ must limit to the real quantity Δ_∞ at high frequency.

In our colloidal system, we can derive a linear relationship between the Fourier components of the average current density $\langle \mathbf{i} \rangle_\omega$ and the average electric field $\langle \mathbf{E} \rangle_\omega$ with the response function being the complex conductivity $K^*(\omega) = K'(\omega) + iK''(\omega)$, that is,

$$\langle \mathbf{i} \rangle_\omega = K^*(\omega) \langle \mathbf{E} \rangle_\omega \tag{6}$$

It might therefore be thought that a Kramers−Kronig relation would exist between $K'(\omega)$ and $K''(\omega)$. However, the conductivity does not have the required high frequency limit discussed above. Recently, for a cell model of the suspension which also has the correct low volume fraction behavior, we have shown[23] that

$$Re(K^*(\omega)) \xrightarrow[\omega \to \infty]{} K_\infty \tag{7}$$

where

$$K_\infty = 3\chi_2 \frac{\kappa^2 k_B T \varepsilon_0 \varepsilon_s}{\bar{\lambda}}$$

and

$$\bar{\lambda}^{-1} = \sum_j \frac{\beta_j}{\lambda_j} \exp\left(- z_j e \Psi^{(0)}(r)/k_B T \right)$$

$$\chi_2 = \frac{-(1+\chi_1\phi)\left(2+\frac{\varepsilon_p}{\varepsilon_s}\right)a^{-3} I_2(a) + 2\chi_1 \left(1-\frac{\varepsilon_p}{\varepsilon_s}\right) a^3 I_{-4}(a)}{\frac{1}{\phi}\left(2+\phi+(1-\phi)\frac{\varepsilon_p}{\varepsilon_s}\right)}$$

$$\chi_1 = \frac{-\left(1-\frac{\varepsilon_p}{\varepsilon_s}\right)}{2+\phi+(1-\phi)\frac{\varepsilon_p}{\varepsilon_s}}$$

and

$$I_n(r) = \int_r^b dr\, r^n \sum_j \frac{\beta_j}{L_j} \exp\left(- z_j e \Psi^{(0)}(r)/k_B T \right)$$

where e, ε_s, ε_p, ε_0, k_B, and T are the electron charge, the relative fluid dielectric permittivity, relative particle dielectric permittivity, vacuum permittivity, Boltzmann constant, and temperature. In addition, z_j and λ_j are the valency and drag coefficient of the jth ion type ($j = 1,2,...,N$), respectively. The equilibrium electrostatic potential within the cell is denoted $\Psi^0(r)$, $b = a/\phi^{1/3}$ is the cell radius, and the parameters β_j and L_j are given by

$$\beta_j = \frac{z_j^2 n_j^\infty}{\sum_j z_j^2 n_j^\infty} \quad \text{and} \quad L_j = -\frac{\lambda_j}{\bar{\lambda}}$$

where n_j^∞ is the (reservoir) ion density. (In the notation of ref 23, $\chi_2 = id_3$, $\chi_1 = d_1$, and $L_j = -iL_j$.) The Debye screening length κ^{-1} is given by

$$\kappa^2 = \sum_{j=1}^N \frac{e^2 z_j^2 n_j^\infty}{\varepsilon_s \varepsilon_0 k_B T}$$

The high frequency limit of the imaginary part of the complex conductivity is [23]

$$\mathrm{Im}(K^*(\omega)) \xrightarrow[\omega \to \infty]{} -\varepsilon_0 \varepsilon_\infty \omega \tag{8}$$

where

$$\varepsilon_\infty = \varepsilon_s(3\chi_1\phi + 1)$$

so $K^*(\omega)$ does not limit to a constant as required for a Kramers−Kronig relation to exist between its real and imaginary parts. This implies that a causal relationship of the type (4) cannot be written between the real current density $\langle \mathbf{i} \rangle(t)$ and the real electric field $\langle \mathbf{E} \rangle(t)$. It is possible to define a related real quantity which does bear the required causal relation with the field. We consider the quantity

$$\mathbf{q}(t) = \frac{1}{\varepsilon_0} \int_{-\infty}^t dt' \langle \mathbf{i} \rangle(t') \tag{9}$$

and contemplate the existence of a causal relation

$$\mathbf{q}(t) = \xi_\infty \langle \mathbf{E} \rangle(t) + \int_{-\infty}^t dt'\, \Xi(t-t') \langle \mathbf{E} \rangle(t') \tag{10}$$

Taking the Fourier transform of eq 9, we obtain

$$\mathbf{q}_\omega = -\frac{1}{i\omega\varepsilon_0} \langle \mathbf{i} \rangle_\omega = \xi(\omega) \langle \mathbf{E} \rangle_\omega \tag{11}$$

where

$$\xi(\omega) = \xi_\infty + \int_0^\infty dt\, \Xi(t)\, e^{i\omega t}$$

Comparison of eqs 11 and 6 shows that

$$\xi(\omega) = \frac{i}{\omega\varepsilon_0} K^*(\omega) \tag{12}$$

and, from eqs 7 and 8, we see that

$$\xi(\omega) \xrightarrow[\omega \to \infty]{} \varepsilon_\infty \tag{13}$$

Hence, the real and imaginary parts of the response function $\xi(\omega)$ will obey a Kramers−Kronig relation. Because $K^*(0) = Re(K^*(0)) = K(0)$ (where $K(0)$ is the zero frequency conductivity of the suspension), it follows from eq 12 that the response function $\xi(\omega)$ has a simple pole at $\omega = 0$ and the Kramers−Kronig result 5 must be modified in this case[22] to read

$$\xi'(\omega) - \xi_\infty = \frac{2}{\pi} P \int_0^\infty dx \frac{x\xi''(x)}{x^2 - \omega^2}$$

$$\xi''(\omega) = -\frac{2\omega}{\pi} P \int_0^\infty dx \frac{\xi'(x) - \xi_\infty}{x^2 - \omega^2} + \frac{K(0)}{\varepsilon_0 \omega} \tag{14}$$

Thus, we see that the process used by Carrique et al.[20] to identify the dielectric response function $\varepsilon(\omega)$ yields the result reported due to the Kramers−Kronig relationship between the components of the response function $\xi(\omega)$, for it follows from eq 12 that

$$\xi'(\omega) = \varepsilon'_{\mathrm{Hist}}(\omega) = -\frac{\mathrm{Im}(K^*(\omega))}{\omega\varepsilon_0}$$

and hence from eq 14 that

$$\xi''(\omega) = \varepsilon''_{\mathrm{Hist}}(\omega) + \frac{K(0)}{\varepsilon_0 \omega}$$

Thus, from eq 12,

$$Re(K^*) = \omega\varepsilon_0\xi''(\omega) = \omega\varepsilon_0\varepsilon''_{\mathrm{Hist}}(\omega) + K(0) \qquad (15)$$

The frequency independent residual constructed by Carrique et al.,[20] eq 3, does not imply that the conduction current component of the conductivity is the zero frequency value for all frequencies. Rather, the Carrique et al.[20] construction cannot fail to yield $K(0)$ in view of eq 15.

We note in passing that the *correct* causal relationship between $\langle \mathbf{i} \rangle(t)$ and $\langle \mathbf{E} \rangle(t)$ is

$$\langle \mathbf{i} \rangle(t) = \varepsilon_0 \left[\xi_\infty \frac{\mathrm{d}\langle \mathbf{E} \rangle(t)}{\mathrm{d}t} + \Xi(0)\, \langle \mathbf{E} \rangle(t) + \int_{-\infty}^{t} \mathrm{d}t' \, \frac{\mathrm{d}\Xi(t-t')}{\mathrm{d}t} \langle \mathbf{E} \rangle(t') \right]$$

obtained by differentiating eq 10 with respect to time.

In what follows, we will correctly identify the dielectric response function for the suspension and determine the frequency dependence of the conduction current.

3. The Dielectric Response of a Colloidal Dispersion

The identification of the dielectric response function must follow from the causal relationship between the real average electric displacement $\langle \mathbf{D} \rangle(t)$ and the real average electric field $\langle \mathbf{E} \rangle(t)$, that is,

$$\langle \mathbf{D} \rangle(t) = \varepsilon_0 \langle \mathbf{E} \rangle(t) + \langle \mathbf{P} \rangle(t) \qquad (16)$$

where the average polarization (dipole moment density) $\langle \mathbf{P} \rangle(t)$ is given by

$$\langle \mathbf{P} \rangle(t) = \varepsilon_0 \int_{-\infty}^{t} \mathrm{d}t' \, \chi(t-t') \, \langle \mathbf{E} \rangle(t') \qquad (17)$$

Here, $\chi(t)$ is the decay function which determines how much of the instantaneously induced dipole density caused by the applied field at a time t in the past still remains at the present time under the action of the inter- and intramolecular relaxation processes of the system. The Fourier transforms of eqs 16 and 17 yield

$$\langle \mathbf{D} \rangle_\omega = \varepsilon_0 \langle \mathbf{E} \rangle_\omega + \langle \mathbf{P} \rangle_\omega$$

$$\langle \mathbf{P} \rangle_\omega = \varepsilon_0 \big(\varepsilon(\omega) - 1 \big) \langle \mathbf{E} \rangle_\omega \qquad (18)$$

where

$$\varepsilon(\omega) = 1 + \int_0^\infty \mathrm{d}t \, \chi(t) \, \mathrm{e}^{i\omega t} \qquad (19)$$

so that the dielectric response function $\varepsilon(\omega)$ appears as the proportionality constant in the linear relationship between the Fourier components of electric displacement and electric field

$$\langle \mathbf{D} \rangle_\omega = \varepsilon_0 \varepsilon(\omega) \langle \mathbf{E} \rangle_\omega$$

as required. To identify $\varepsilon(\omega)$, we must derive the linear relation between the Fourier components of the polarization and the electric field.

The average polarization has two components. The first is the induced dipole moment density arising from the polarization of the dielectric continuum of the medium and the particles

$$\langle \mathbf{P_D} \rangle_\omega = \left\langle -\frac{1}{V} \int_V dV \big(\varepsilon(\mathbf{r}) - \varepsilon_0 \big) \nabla \Psi^{(1)}(\mathbf{r}) \right\rangle \qquad (20)$$

where $\Psi^{(1)}(\mathbf{r}) \mathrm{e}^{-i\omega t}$ is the local perturbation electrostatic potential,

$$\varepsilon(\mathbf{r}) = \begin{cases} \varepsilon_\mathrm{p}\varepsilon_0 & \mathbf{r} \subset V_\mathrm{p} \\ \varepsilon_\mathrm{s}\varepsilon_0 & \mathbf{r} \subset V_\mathrm{f} \end{cases}$$

and V_p and V_f are the particle and fluid volumes of the suspension (with particle volume fraction $\phi = V_\mathrm{p}/(V_\mathrm{p} + V_\mathrm{f})$).

The second contribution is the charge polarization

$$\langle \mathbf{P_C} \rangle_\omega = \left\langle -\frac{1}{V} \int_V \mathrm{d}V \, \rho_{\mathrm{ch}}^{(1)} \mathbf{r} \right\rangle \qquad (21)$$

where $\rho_{\mathrm{ch}}^{(1)} \mathrm{e}^{-i\omega t}$ is the local perturbation charge density in the presence of the applied field. In the cell model treatment of the concentrated suspension, the particle occupies the central region $r < a$ of the cell and the fluid the region $a < r < b$ where the particle volume fraction $\phi = (a/b)^3$.

The dielectric contribution eq 20 can be written

$$\langle \mathbf{P_D} \rangle_\omega = -\frac{\varepsilon_0}{V_{\mathrm{cell}}} \left[\int_{V_\mathrm{p}} \mathrm{d}V (\varepsilon_\mathrm{p} - 1) \nabla \Psi^{(1)}(\mathbf{r}) + \int_{V_\mathrm{f}} \mathrm{d}V (\varepsilon_\mathrm{s} - 1) \nabla \Psi^{(1)}(\mathbf{r}) \right]$$

Recognizing that $\nabla \cdot (\psi(r)\mathbf{I}) = \nabla\psi(r)$ (where $\mathbf{I}$ is the unit dyadic), we may write

$$\langle \mathbf{P_D} \rangle_\omega = -\frac{\varepsilon_0}{V_{\mathrm{cell}}} \left[(\varepsilon_\mathrm{p} - 1) \int_{S_\mathrm{p}^-} \mathrm{d}S \hat{\mathbf{r}} \, \Psi^{(1)}(\mathbf{r}) + (\varepsilon_\mathrm{s} - 1) \left(\int_{S_{\mathrm{cell}}} \mathrm{d}S \hat{\mathbf{r}} \, \Psi^{(1)}(\mathbf{r}) - \int_{S_\mathrm{p}^+} \mathrm{d}S \hat{\mathbf{r}} \, \Psi^{(1)}(\mathbf{r}) \right) \right]$$

with the aid of Green's theorem. Invoking the symmetry of the cell model system

$$\Psi^{(1)}(\mathbf{r}) = \psi(r) \langle \mathbf{E} \rangle_\omega \cdot \hat{\mathbf{r}}$$

the surface integrals are evaluated to yield

$$\langle \mathbf{P_D} \rangle_\omega = \varepsilon_0 \left[(\varepsilon_\mathrm{s} - \varepsilon_\mathrm{p}) \phi \, \frac{\psi(a)}{a} + (\varepsilon_\mathrm{s} - 1) \right] \langle \mathbf{E} \rangle_\omega$$

where we have used the cell boundary condition[14]

$$\psi(b) = -b$$

In the cell model, the charge polarization contribution eq 21 is

$$\langle \mathbf{P_C} \rangle_\omega = \left\langle -\frac{1}{V_{\mathrm{cell}}} \int_{V_\mathrm{f}} \mathrm{d}V \, \rho_{\mathrm{ch}}^{(1)} \mathbf{r} \right\rangle \qquad (22)$$

since there is no charge density inside the particle. Using Poisson's equation

$$\rho_{\mathrm{ch}}^{(1)}(\mathbf{r}) = -\varepsilon_0 \varepsilon_s \nabla \cdot \nabla \Psi^{(1)}(\mathbf{r})$$

and the identity $\nabla\cdot\nabla\Psi^{(1)}\mathbf{r} = \nabla\cdot(\nabla\Psi^{(1)}\mathbf{r}) - \nabla\Psi^{(1)}$, we may write eq 22 as

$$\langle\mathbf{P_C}\rangle_\omega = -\frac{\varepsilon_0\varepsilon_s}{V_{cell}}\left[\int_{S_{cell}} dS\hat{\mathbf{r}}\cdot\nabla\Psi^{(1)}\mathbf{r} - \int_{S_p^+} dS\hat{\mathbf{r}}\cdot\nabla\Psi^{(1)}\mathbf{r} - \int_{V_f} dV\nabla\Psi^{(1)}\right]$$

with the aid of Green's theorem. From the symmetry of $\Psi^{(1)}(\mathbf{r})$, we have

$$\hat{\mathbf{r}}\cdot\nabla\Psi^{(1)}(\mathbf{r}) = \frac{d\psi}{dr}\langle\mathbf{E}\rangle_\omega\cdot\hat{\mathbf{r}}$$

so that

$$\langle\mathbf{P_C}\rangle_\omega = -\varepsilon_0\varepsilon_s\left[\frac{d\psi}{dr}(b)\langle\mathbf{E}\rangle_\omega - \phi\frac{d\psi}{dr}(a^+)\langle\mathbf{E}\rangle_\omega - \frac{1}{V_{cell}}\left(\int_{V_{cell}} dV\nabla\Psi^{(1)} - \int_{V_p} dV\nabla\Psi^{(1)}\right)\right] \quad (23)$$

By definition

$$\langle\mathbf{E}\rangle_\omega = -\frac{1}{V_{cell}}\int_{V_{cell}} dV\nabla\Psi^{(1)}$$

and the last term in eq 23 was evaluated above. Hence, we may write

$$\langle\mathbf{P_C}\rangle_\omega = -\varepsilon_0\varepsilon_s\left[1 + \frac{d\psi}{dr}(b) - \phi\left(\frac{d\psi}{dr}(a^+) - \frac{\psi(a)}{a}\right)\right]\langle\mathbf{E}\rangle_\omega \quad (24)$$

The boundary condition on $\psi(r)$ at the particle surface is[14]

$$\frac{d\psi}{dr}(a^+) = \frac{\varepsilon_p}{\varepsilon_s}\frac{\psi(a)}{a}$$

so that eq 24 becomes

$$\langle\mathbf{P_C}\rangle_\omega = \left[-\varepsilon_0\varepsilon_s\left(1 + \frac{d\psi}{dr}(b)\right) + \varepsilon_0\phi(\varepsilon_p - \varepsilon_s)\frac{\psi(a)}{a}\right]\langle\mathbf{E}\rangle_\omega$$

The total polarization is then

$$\langle\mathbf{P}\rangle_\omega = \varepsilon_0\left[-\varepsilon_s\frac{d\psi}{dr}(b) - 1\right]\langle\mathbf{E}\rangle_\omega$$

and the dielectric response function for the cell model suspension is, from eq 18,

$$\varepsilon(\omega) = -\varepsilon_s\frac{d\psi}{dr}(b) \quad (25)$$

Note that the potential gradient term in eq 25 has both real and imaginary parts because the perturbation potential arises from a complex applied field $\langle\mathbf{E}\rangle_\omega e^{-i\omega t}$, so that

$$\varepsilon'(\omega) = -\varepsilon_s Re\left(\frac{d\psi}{dr}(b)\right) \quad \text{and}$$

$$\varepsilon''(\omega) = -\varepsilon_s Im\left(\frac{d\psi}{dr}(b)\right) \quad (26)$$

We will display these components of $\varepsilon(\omega)$ in the next section.

Additional proof that this definition of the dielectric response function of the cell model suspension is the correct one comes from the cell model expression for the complex conductivity,[16]

$$K^*(\omega) = -\rho_{ch}^{(0)}(b)\mu\phi\frac{\Delta\rho}{\rho_s} + \sum_{j=1}^{N}\frac{z_j^2e^2n_j^{(0)}(b)}{\lambda_j}\frac{d\phi_j}{dr}(b) + i\omega\varepsilon_0\varepsilon_s\frac{d\psi}{dr}(b) \quad (27)$$

where μ is the dynamic mobility and $\Delta\rho = \rho_p - \rho_s$, where ρ_s and ρ_p are the mass densities of the fluid and particle, respectively. The equilibrium ion density is

$$n_j^{(0)}(r) = n_j^\infty\exp\left(-z_je\Psi^{(0)}(r)/k_BT\right)$$

and ϕ_j is the perturbation to the electrochemical potential resulting from application of the electric field. All we need from this equation is the knowledge that, in the derivation of eq 27, the first two terms come from the conduction current contribution and the last one comes from the displacement current contribution to the total local current[16] which is then volume averaged to yield eq 6. From eq 25, we see that this displacement current term is just $-i\omega\varepsilon_0\varepsilon(\omega)$ as expected if $\varepsilon(\omega)$ is to be the effective dielectric response of the suspension regarded as a continuum. This term is complex, since the electrostatic potential gradient, $d\psi/dr$, is complex.

One problem remains. From eq 8, we see that $\varepsilon(\omega)\xrightarrow[\omega\to\infty]{}\varepsilon_\infty$. However, the definition of $\varepsilon(\omega)$ in terms of the decay function, $\chi(t)$, eq 19, seems to require that this limit be unity. This difficulty is resolved by allowing an instantaneous polarization response from the movement of the charges in the double layer in addition to the instantaneous electric displacement shown in eq 16. This is achieved by writing

$$\chi(t) = (\varepsilon_\infty - 1)\delta(t) + \beta(t)$$

where $\beta(t)$ is a *finite* decay function. Thus, eq 19 becomes

$$\varepsilon(\omega) = \varepsilon_\infty + \int_0^\infty dt\,\beta(t)\,e^{i\omega t}$$

and therefore a Kramers−Kronig relation between $\varepsilon'(\omega) - \varepsilon_\infty$ and $\varepsilon''(\omega)$ must exist in the form given in eq 5. Note that, at very high frequencies, the imaginary part of the conduction contribution $K''_{cond}(\omega)\xrightarrow[\omega\to\infty]{}0$ so that it is correct to use the high frequency value of the dielectric response function, ε_∞, as calculated in ref 23, in our Kramers−Kronig calculations.

Also, we note in passing that the ion chemical potential gradient functions $d\phi_j(b)/dr$ and the electrophoretic mobility μ in the conduction current contributions to the complex conductivity (eq 27) are *complex quantities*, providing further evidence that the historical assumption that the conduction current is real[1,4,16−21] and the conclusion that it is independent of frequency are both incorrect. As a consequence, it is also incorrect to associate the real part of the dielectric response function with the imaginary part of the complex conductivity (as described in section 1). Unfortunately, this has the corollary that the dielectric response cannot be deconvoluted from the complex conductivity in the manner proposed by Carrique et al.,[20] since *both the real and imaginary components of K*(ω) contain contributions from both the conduction and displacement current terms*. Although we are led to these conclusions by examining the cell model approximation to a real suspension, the cell model limits to the dilute behavior of the Mangelsdorf and White model,[5] which is exact

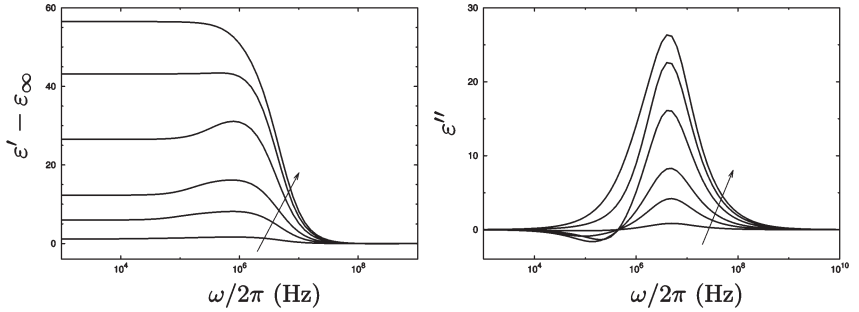

Figure 1. Frequency response of the (a) real and (b) imaginary parts of the dielectric response for various volume fractions, $\phi = 0.01, 0.05, 0.1, 0.2, 0.3$, and 0.4. Arrows show the trends with increasing volume fraction. Reduced ζ potential is $\bar{\zeta} = 4$, and $\kappa a = 10$.

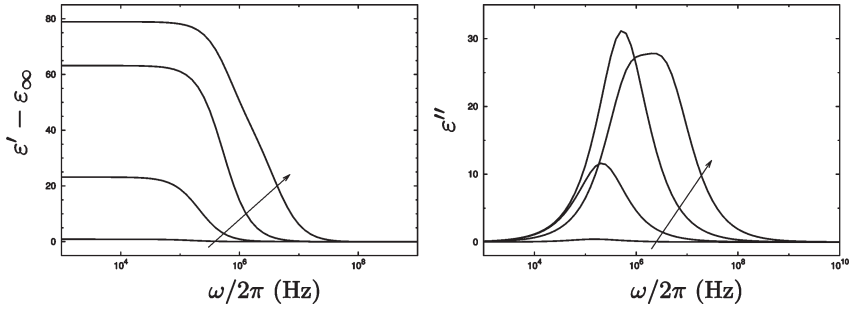

Figure 2. Frequency response of the (a) real and (b) imaginary parts of the dielectric response for various reduced ζ-potentials, $\bar{\zeta} = 1, 4, 7$, and 10. Arrows show the trends with increasing $\bar{\zeta}$. Volume fraction $\phi = 0.1$, and $\kappa a = 1$.

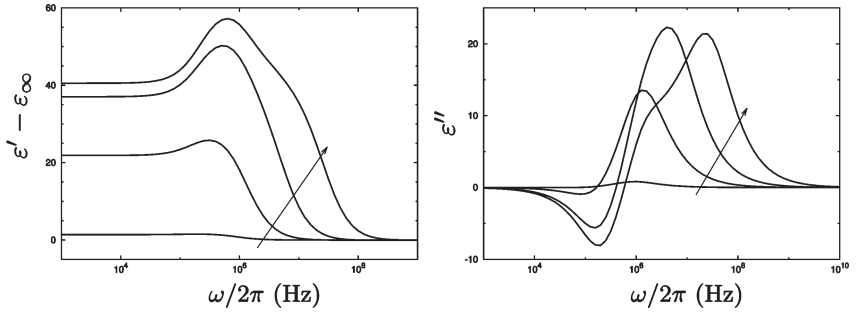

Figure 3. Frequency response of the (a) real and (b) imaginary parts of the dielectric response for various reduced ζ potentials, $\bar{\zeta} = 1, 4, 7$, and 10. Arrows show the trends with increasing $\bar{\zeta}$. Volume fraction $\phi = 0.1$, and $\kappa a = 5$.

within the standard model of colloidal electrokinetics. Hence, the conclusions are likely to be valid, independent of the choice of model.

4. Results and Discussion

In this section, the real and imaginary parts of the actual dielectric response are examined both as functions of frequency and via the use of Cole−Cole plots. For many systems, the imaginary part of the dielectric response is negative for some frequency range, producing interesting Cole−Cole plots. If viewed in isolation, this violates the law of increasing entropy. However, when viewed as a whole, the system is dissipative due to the conductive nature of the medium. We also examine the imaginary part of the conduction contribution, $K''_{\mathrm{cond}}(\omega)$. Finally, we show that we have correctly identified the actual dielectric response by calculating the dielectric memory function and showing that a Kramers−Kronig relationship exists between the real and imaginary parts of the dielectric response. Two relaxation mechanisms, namely, the α and the Maxwell−Wagner relaxations, are also examined. All calculations have been performed with particle size $a = 100$ nm and $\varepsilon_p = 2$, with varying concentrations of KCl solution.

4.1. Dielectric Response. The real and imaginary parts of the dielectric response (eq 26) for a range of volume fractions, double layer thicknesses (κa), and reduced ζ potentials ($\bar{\zeta} = e\zeta/k_B T$) are shown in Figures 1−4.

The figures showing the real part of the dielectric response (part (a)) display trends with increasing volume fraction, ζ potential and double layer thickness. Some of these trends, in particular for low κa and low ζ potential, are similar to those described elsewhere for the imaginary part of the complex conductivity (see for example[1,4,16,17]) and these discussions will not be repeated here. This is particularly true at high frequencies (since $K''_{\mathrm{cond}} \xrightarrow{\omega \to \infty} 0$). However, for more extreme system parameters, the results show a divergence from the traditional plots of $-\mathrm{Im}(K^*(\omega))/\varepsilon_0\omega$ due to the contribution of the frequency dependent imaginary part of the conduction contribution, intrinsically embedded in $\mathrm{Im}(K^*(\omega))$, but traditionally assumed to be zero.

The imaginary part of the dielectric response is shown in part (b) of the figures. Although some features of these curves are similar to those seen in plots of the real part of the complex conductivity (see, e.g. ref 16) or in plots of the incorrectly calculated imaginary part of the dielectric response

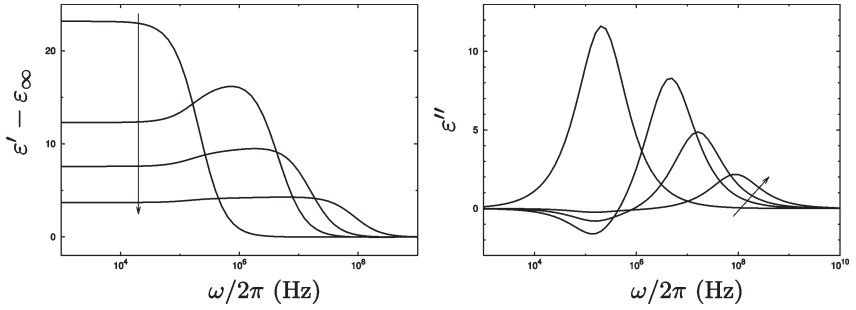

Figure 4. Frequency response of the (a) real and (b) imaginary parts of the dielectric response for various double layer thicknesses, $\kappa a = 1, 10, 20$, and 50. Arrows show the trends with increasing κa value. Reduced ζ potential is $\bar{\zeta} = 4$, and $\phi = 0.1$.

(see, e.g., ref 1), there is one feature which has not been seen before.

In almost all systems where $\kappa a > 1$, there exists a frequency range for which $\varepsilon'' < 0$. For a dielectric medium, the imaginary part of the dielectric response must be positive to ensure the dissipation of energy.[22] Since we are concerned with a conductive medium, this constraint no longer holds, however, since the system, when viewed as a whole, is dissipative and the net entropy increases on application of an external field.

From the figures, it is easy to identify two different relaxation mechanisms. The so-called α-relaxation[25] occurs in the frequency range 10^4-10^6 and is most easily identified in the figures displaying the imaginary part of the dielectric response. This relaxation is associated with the polarization of the double layer and represents the time taken for the particles to diffuse the particle radius and the double layer thickness.[26] For dilute suspensions, the frequency at which this relaxation occurs can be calculated via an expression derived from the standard DeLacey−White[4] model of electrokinetics:

$$\omega_\alpha = \frac{2\pi D}{\left(a+\kappa^{-1}\right)^2} = \frac{2\pi k_B T}{\lambda_{ci}\left(a+\kappa^{-1}\right)^2} \tag{28}$$

where λ_{ci} is the drag coefficient of the counterion.

Despite the fact that this expression is only valid for extremely low volume fractions,[1,17] variations in the relaxation frequency with volume fraction $\phi < 0.5$ are not greater than an order of magnitude,[1] so that eq 28 provides a good estimate of the relaxation frequency for all volume fractions considered here.

The α-relaxation can be seen in Figures 1, 3, and 4 where $\varepsilon'' < 0$. In all cases where $\kappa a = 1$, $\varepsilon'' > 0$ for the entire frequency range. The ion distribution in the system is low, and the system then behaves more dielectric-like.

The Maxwell−Wagner relaxation[26] occurs at a higher frequency and is identifiable in both the real and imaginary parts of the dielectric response. This relaxation is associated with the discontinuity of the conductivity and permittivity at the surface of the particles. It is represented by the sharp increase in the imaginary part of the dielectric response. The frequency at which the relaxation occurs can be calculated via[1]

$$\omega_{MW} = \frac{K_{sol}}{\varepsilon_s\varepsilon_0}\frac{2(1-\phi)Du+2+\phi}{2+\phi} \tag{29}$$

where K_{sol} is the conductivity contribution from the bulk electrolyte at zero frequency,

$$K_{sol} = \sum_j \frac{z_j^2 e^2 n_j^\infty}{\lambda_j}$$

and for a symmetric electrolyte, $z_1 = -z_2 = z$ and $\lambda_1 = \lambda_2 = \lambda$,[24] the Dukhin number is

$$Du = \frac{K^S}{K_{sol}a} = \frac{1}{\kappa a}\exp\left(\frac{ez\zeta}{2k_BT}\right)\left(1+3\frac{m}{z^2}\right)$$

where

$$m = \frac{2\varepsilon_0\varepsilon_s k_B T\lambda}{2\eta_s e^2}$$

The Maxwell−Wagner relaxation frequency (eq 29) is accurate for thin double layer suspensions. For thick double layer systems, K^S, which describes the "surface conduction" due to the movement of ions in the double layer, is not well-defined. However, for the parameters used in this paper, the Dukhin number $Du \ll 1$ so that

$$\omega_{MW} = \frac{K_{sol}}{\varepsilon_0\varepsilon_s} \tag{30}$$

is a good approximation and has been used for the calculations in this paper.

Figures 1b−3b show that the frequency at which the imaginary part of the dielectric response begins to increase is largely independent of the volume fraction and ζ potential. On the other hand, the Maxwell−Wagner relaxation frequency is dependent on κ (as expected from eq 30) as demonstrated in Figure 4b. The increase in relative displacement of the two relaxation frequencies with increased κa, shown in Figure 4b, is consistent with the generic analysis of Shilov et al.[21] who argued that

$$\omega_{MW} \sim (\kappa a)^2 \omega_\alpha$$

That is, where the α-relaxation frequency appears insensitive to κa, the Maxwell−Wagner frequency shifts to higher frequencies.

While our model includes no explicit treatment of surface conductivity, when the ζ potential is extremely high (e.g., in Figure 3), it does discriminate between the properties of the inner and outer double layer regions. With reason, this discrimination affects the α-relaxation process more than the Maxwell−Wagner relaxation. The ions, which are predominantly, if not exclusively the counterions, in the inner region of the double layer will

(24) O'Brien, R. W. *J. Colloid Interface Sci.* **1986**, *113*, 81.
(25) Shilov, V. N.; Delgado, A. V.; González-Cabellero, F.; Grosse, C.; Donath, E. In *Interfacial Electrokinetics and Electrophoresis*; Delgado, A. V., Ed.; Dekker: New York, 2002; Chapter 12, pp 329−368.
(26) Dukhin, S. S.; Shilov, V. N. *Dielectric phenomena and the double layer in disperse systems and polyelectrolytes*; Wiley: New York, 1974.

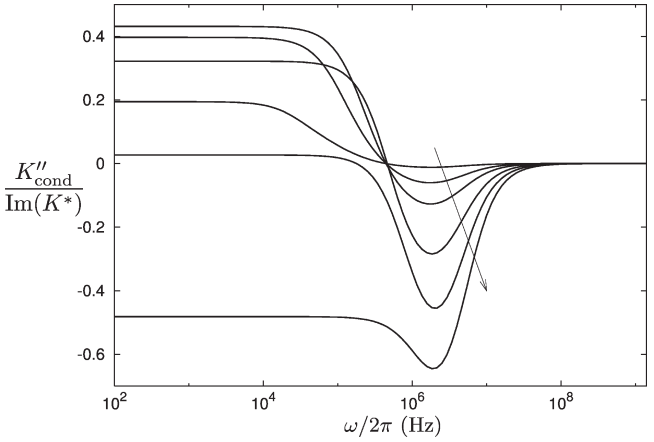

Figure 5. Frequency response of the imaginary part of the conduction current contribution to the complex conductivity, $K''_{cond}(\omega)$, as a fraction of the imaginary part of the complex conductivity, $Im(K^*(\omega))$. Arrow shows the trend with increasing volume fraction, $\phi = 0.01$, 0.05, 0.1, 0.2, 0.3, and 0.4. Reduced ζ potential is $\bar{\zeta} = 4$, and $\kappa a = 10$.

experience their own relaxation, distinct from the relaxation occurring in the outer, more diffuse, double layer normally recognized as the α-relaxation phenomenon. This effect is likely a contributing factor to the appearance in Figure 3 of an additional relaxation frequency for the highest ζ potential ($\bar{\zeta} = 10$). Note, however, that incorporation of finite ion size would alter the appearance of this phenomenon.

4.2. Conduction Current Contribution to the Complex Conductivity. From eq 27 it follows that the conduction current contribution to the complex conductivity is

$$K^*_{cond}(\omega) = -\rho^{(0)}_{ch}(b)\mu\phi\frac{\Delta\rho}{\rho_s} + \sum_{j=1}^{N}\frac{z_j^2e^2n_j^{(0)}(b)}{\lambda_j}\frac{d\phi_j}{dr}(b) \quad (31)$$

In Figure 5 we plot the imaginary part of this quantity, $K''_{cond}(\omega)$, as a fraction of the entire imaginary part of the complex conductivity, $Im(K^*(\omega))$, for a range of volume fractions and a typical ζ potential and double layer thickness (κa).

In contrast to the historical approach where K''_{cond} is assumed zero, Figure 5 shows that $K''_{cond}(\omega)$ is nonzero, strongly frequency dependent, and moreover, a significant fraction of the imaginary part of the complex conductivity except at very high frequencies. In the high frequency range, $K''_{cond}(\omega)$ approaches zero (in absolute value, and as a fraction of the total $Im(K^*(\omega))$). At low frequencies, the ratio of $K''_{cond}(\omega)$ to $Im(K^*(\omega))$ is a constant as both quantities approach zero at the same rate with decreasing frequency.

4.3. Cole−Cole Plots for the Dielectric Response. Figures 6−9 show Cole−Cole plots[27] for the complex dielectric response (eq 26), in which the imaginary part of the dielectric response is plotted as a function of the real part. Frequency increases in an anticlockwise direction. The α and Maxwell−Wagner relaxation frequencies calculated via eqs 28 and 30 are shown with filled and open triangles, respectively. As a point of reference from which to understand these figures, a Cole−Cole plot for a physical quantity, with a response function that can be represented by a single exponential decay (with only one characteristic relaxation frequency), would be semicircular.

(27) Cole, K. S.; Cole, R. H. *J. Chem. Phys.* **1941**, *9*, 341.

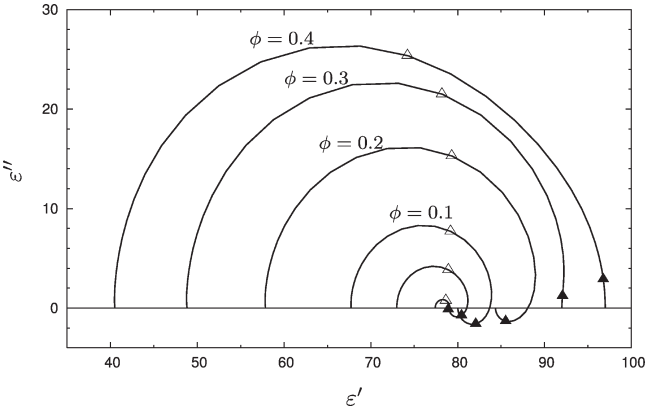

Figure 6. Cole−Cole plot for the dielectric response for various volume fractions, $\phi = 0.01$, 0.05, 0.1, 0.2, 0.3, and 0.4. Arrows show trends with increasing volume fraction. Reduced ζ potential is $\bar{\zeta} = 4$, and $\kappa a = 10$. Frequency increases in an anticlockwise direction. Filled triangles show the α relaxation frequency, and open triangles show the Maxwell−Wagner relaxation frequency.

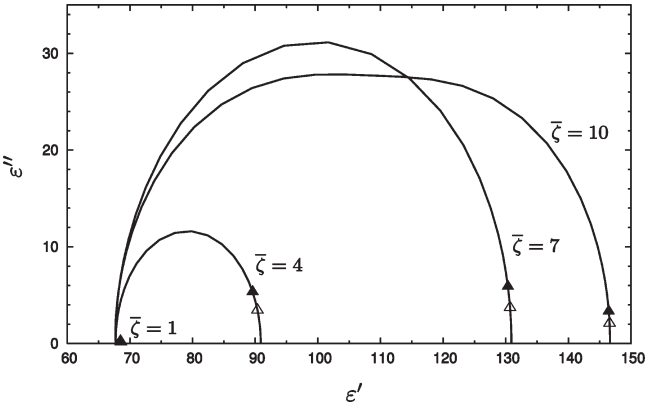

Figure 7. Cole−Cole plot for the dielectric response for various reduced ζ potentials, $\bar{\zeta} = 1$, 4, 7, and 10. Arrows show trends with increasing $\bar{\zeta}$. Volume fraction $\phi = 0.1$, and $\kappa a = 1$. Frequency increases in an anticlockwise direction. Filled triangles show the α relaxation frequency, and open triangles show the Maxwell−Wagner relaxation frequency.

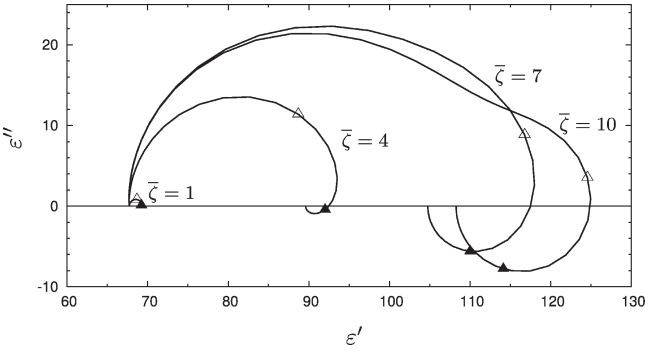

Figure 8. Cole−Cole plot for the dielectric response for various reduced ζ-potentials, $\bar{\zeta} = 1$, 4, 7, and 10. Arrows show trends with increasing $\bar{\zeta}$. Volume fraction $\phi = 0.1$, and $\kappa a = 5$. Frequency increases in an anticlockwise direction. Filled triangles show the α relaxation frequency, and open triangles show the Maxwell−Wagner relaxation frequency.

For systems with thick double layers (where $\kappa a = 1$ or smaller), the two relaxation frequencies become very close. However, the equation used to calculate the Maxwell−Wagner relaxation

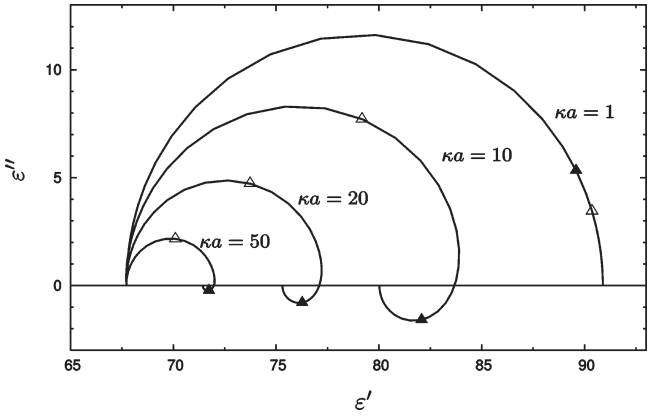

Figure 9. Cole−Cole plot for the dielectric response for various double layer thicknesses, κa = 1, 10, 20, and 50. Arrows show trends with increasing κa value. Reduced ζ potential is $\bar{\zeta}$ = 4, and ϕ = 0.1. Frequency increases in an anticlockwise direction. Filled triangles show the α relaxation frequency, and open triangles show the Maxwell−Wagner relaxation frequency.

frequency, given by either eq 29 or 30 is not accurate in this regime. Similarly, for very large volume fractions, the equation for the α relaxation frequency is less accurate since it is derived from a model for dilute suspensions. In both of these cases, the Cole−Cole plots are near semicircular.

In all other cases, the Cole−Cole plots are not semicircular. Rather, they are approximately represented by the superposition of two semicircles: one above the real axis and one below. These shapes are characteristic of a response exhibiting two distinct relaxation frequencies rather than a distribution of relaxation frequencies. In these cases, the response function can be approximated by the sum of two exponentials each with a different characteristic frequency.

4.4. Dielectric Memory Function. The dielectric response function, $\beta(t)$, can be obtained by calculating the inverse Fourier cosine transform of the real part of the dielectric response or the inverse sine transform of the imaginary part of the dielectric response (eq 26):

$$\beta(t) = \frac{2}{\pi}\int_0^\infty \mathrm{d}\omega\left[\varepsilon'(\omega) - \varepsilon_\infty\right]\cos(\omega t) \tag{32}$$

or

$$\beta(t) = \frac{2}{\pi}\int_0^\infty \mathrm{d}\omega\,\varepsilon''(\omega)\sin(\omega t) \tag{33}$$

In Figure 10, we display the memory function for a near semicircular Cole−Cole plot system (one relaxation time) (line a) and three two semicircular Cole−Cole plot systems (two relaxation times) (lines b−d).

The values calculated for the dielectric memory function via the inverse sine transform (eq 33) are indistinguishable from those obtained via the inverse cosine transform (eq 32). This is proof that a Kramers−Kronig relationship exists between the real and imaginary parts of the dielectric response and direct evidence that we have correctly identified its form.

The line for the near semicircular Cole−Cole plot system (line a) is straight, indicating that the dielectric memory function can be expressed as a single exponential with a single characteristic relaxation frequency. For systems that result in a Cole−Cole plot with a two semicircular shape (curves b−d), the curves are made up of two straight lines, suggesting that the dielectric memory

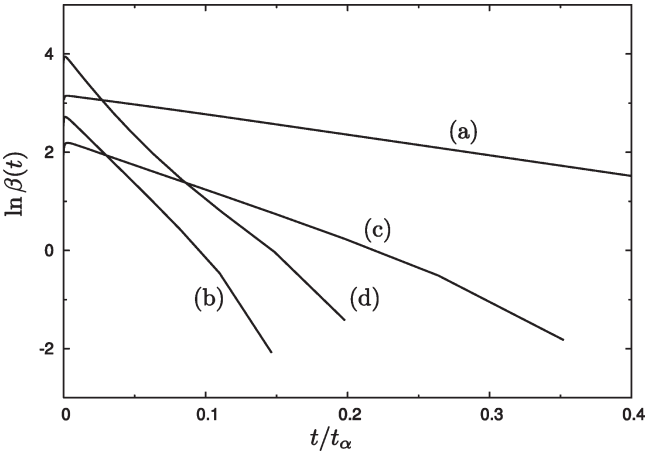

Figure 10. Log of the dielectric memory function, ln $\beta(t)$, for various systems. Calculations using eqs 32 and 33 yield the same results. (a) Near semicircular Cole−Cole plot system: $\bar{\zeta}$ = 4, κa = 1, ϕ = 0.1. (b−d) Two semicircular Cole−Cole plot systems: (b) $\bar{\zeta}$ = 4, κa = 10, ϕ = 0.1; (c) $\bar{\zeta}$ = 4, κa = 5, ϕ = 0.1; (d) $\bar{\zeta}$ = 7, κa = 5, ϕ = 0.1.

function can be expressed as the sum of two exponential functions with two different characteristic relaxation frequencies.

5. Summary Remarks

At high frequencies, the experimental determination of the dielectric response of a dense colloidal suspension has the potential to be an accurate means of studying electrokinetic behavior. First, at high frequencies, experimental artifacts are minimized, and, second, both real and imaginary parts are comparable in magnitude. What we have provided in this paper is a self-contained theoretical review of the dielectric response, established within the framework of a cell model, with which to interpret such experiments.

Particular attention has been paid to the mathematical connection between the real and imaginary parts of the dielectric response. We have derived, from first principles, an expression for the actual dielectric response of a system and demonstrated that it obeys a Kramers−Kronig relationship. We have thereby clarified the historical view (see refs 1, 4, 16−21, and others) that the conduction current was entirely real and independent of frequency.

We have demonstrated that the imaginary part of the conduction current contribution to the complex conductivity is not zero; that is, *the conduction current contribution to the complex conductivity is not directly in phase with the applied field*. The complex conductivity should be written as the sum of two contributions, the conduction current contribution and the displacement current contribution, *both of which are complex*, see eq 1. The implication of this is that it is incorrect to identify the real part of the dielectric response, $\varepsilon'(\omega)$, with the imaginary part of the complex conductivity, Im($K^*(\omega)$), as is traditionally done.[1,4,16−21] In addition, this means that experimentally we cannot identify the real part of the actual dielectric response, $\varepsilon'(\omega)$, and hence $\varepsilon''(\omega)$ unambiguously.

In plotting the actual dielectric response of a system, the real and imaginary parts as a function of frequency as well as against each other in a Cole−Cole style plot, we have established that both contributing parts exhibit characteristics of two relaxation phenomena: the Maxwell−Wagner and the α-relaxations. However, the imaginary part generally is the more sensitive instrument. Moreover, we have found that for $\kappa a > 1$, the system

can have a dielectric response that possesses a negative imaginary part, characteristic of a conducting medium. The frequency range over which this occurs generally encompasses the α-relaxation process.

The inverse Fourier transform of the simulated dielectric response has been compared with a phenomenological dielectric response function composed of two exponential decays, differing in characteristic decay times. Reasonable agreement over several orders of magnitude in time between the simulations and the phenomenological form has been found. The fitted decay times also compare well with the times extracted from the explicit simulations.